Preparation of Spherical Sub-Micron Alumina from Hainan Kaolin

Kai Xu, Jiafei Li, Yongming Zhang*

Hainan Provincial Fine Chemical Engineering Research Center, Hainan University, Hainan, China

**Corresponding Author.*

Abstract

It is an effective way to prepare alumina by replacing bauxite with aluminous minerals. It was studied that the preparation of spherical sub-micron alumina from Hainan kaolin by alginate assisted dispersion. The results of the experiment showed that the alumina content in Hainan kaolin is more than 38%. The t process parameters as of extracting alumina by acid leaching were optimized by uniform design optimization method. The alumina extraction rate reached more than 97% with optimized process conditions. It was used as aluminum source material that he aluminum salt obtained from Hainan kaolin was treated with impurity removal. With this source material, and the purified alginate AG was used as dispersant, the α- Alumina powder with good sphericity, uniform dispersion and average particle size of about 350 was prepared.

Keywords: *Hainan kaolin, acid leaching method, AG dispersant; spherical α-Al2O3*

I. Introduction

China has the world's largest aluminum industry, but lacks aluminum ore resources, with dependence on bauxite imports reaching as high as 50%[1,2]. Only in 2018, the import volume reached 87 million tons, but China has rich kaolin ore reserves which rank the second in the world [3]. Al2O3 content in the composition of pure kaolin is as high as 45% (burning base), which is an ideal alternative source of bauxite [3-4]. The Hainan kaolin mine has a late discovery, whose reserves are medium-sized mines with initial development and utilization. Where, the Hainan Baoluo mine, which is characterized by soft sandy kaolin containing quartz sand prone to washing and separation, has a high development value. The exploration and research on the preparation of special alumina from Hainan kaolin carries great practical significance for broadening the application fields of local mineral resources and increasing the economic added value of local resources.

Alumina is the basic raw material for metal aluminum, chemical and optoelectronic materials. Where, electronic grade alumina is widely used in phosphors, lithium battery electrodes, LED lamp substrates, laser window glass sapphire, integrated circuit board substrates and other optoelectronic materials[6 ,7]. With the development of electronic components and integrated circuits towards miniaturization and high integration, more stringent requirements are raised for the purity and particle morphology of raw material alumina, and increasingly higher requirements are raised for the sphericity and particle size uniformity of alumina particles to improve the uniformity and density of alumina in electronic products. For high-purity submicron alumina prepared by traditional electronic grade alumina preparation methods such as solid phase method, gas phase method, liquid phase method, etc. [6,8-10], its particle sphericity (such as rod, ellipsoid) and particle size uniformity is not ideal.

This paper takes Hainan kaolin as the raw material and the aluminum salt AlCl3 extracted by acid method as the aluminum source, adopts AG-assisted dispersion method to improve the sphericity and particle uniformity of alumina particles, thereby investigating the effect of reaction conditions such as reaction temperature, reaction time, and dispersant action on the product performance, and exploring the auxiliary dispersion mechanism of AG.

ISSN: 0010-8189

II. Experimental Part

2.1 Experimental materials

Hainan kaolin (HN19), taken from a kaolin company in Wenchang, Hainan, is primary water selection; for purified alginate AG, dried red algae plants were processed by alkali treatment, bleaching, acidification, and boiling to obtain primary red algae; use ammonia water to adjust the 5% NH4Cl solution to pH7, wash the primary red algae with NH4Cl solution 3 times, float off the suspended impurities in the upper layer, and then filter to obtain the purified product AG with a loss on drying <15%; dispersants hexadecyl trimethyl ammonium bromide, sodium dodecyl benzene sulfonate, polyvinylpyrrolidone, etc. were all of AR grade, which were purchased from Macklin Biochemical Technology Co., Ltd.

2.2 Analysis and testing

Phase analysis was carried out with Dandong Instrument's Y2000 polycrystalline X-ray diffractometer under CuKα ray/30Kv/25mA, scanning speed 0.05°/s; BET analysis was carried out using ASAP2460 physical adsorption instrument from Mike Company, and Baxter BT-9300H laser particle analyzer was used to measure the aggregate particle size of the sample; the SU8020 electron microscope of Hitachi, Japan was used to observe the particle size and morphology of the primary particles.

2.3 Preparation of aluminum salt solution by acid leaching of kaolin and its removal of impurities

Hydrochloric acid solution of a certain concentration and activated kaolin were respectively added to a polytetrafluoroethylene lined autorotating reactor, and leached at a certain speed and temperature. After the reaction, the leaching solution A and the filter cake were separated by filtering separation; the filter cake was washed with hydrochloric acid of a certain concentration, and the washing mother liquor B was poured into the leaching solution A to obtain the leaching solution C (aluminum chloride solution).

HCl gas was admitted into the leaching solution C for salt precipitation reaction. When the HCl in the solution reached more than 30%, AlCl3•6H2O crystals would precipitate out, and other metal impurities would remain in the concentrated hydrochloric acid solution to obtain purified AlCl3•6H2O crystals [11]. Purification was repeated 3 times. Dissolve the purified AlCl3•6H2O crystals, then add a certain amount of ammonium sulfate, adjust the slightly alkaline pH with ammonia water to further precipitate and remove impurities [12]. After reaction at a certain temperature for a certain time, ammonium aluminum sulfate crystals NH4Al(SO4)2•24H2O were precipitated for further removal after hot filtration and filtrate cooling.

2.4 Preparation of spherical submicron alumina

Add aluminum ammonium sulfate and urea at a certain proportion into a proper amount of distilled water, make it completely dissolve via ultrasonography, then add a certain amount of AG glue, fully stir to make it completely dissolve, and then transfer it to a PTFE-lined autorotating reactor. The filling degree was less than 70% to prevent expansion. Let it react at a certain temperature for a certain time and then cool to room temperature naturally. Obtain the intermediate product filter cake through filtration and use distilled water and absolute ethanol to ultrasonically cross-wash the filter cake several times to obtain submicron alumina precursor through freeze drying. After mechanical grinding, the precursor was calcined at a certain temperature for a certain period of time to obtain spherical submicron alumina.

III Experimental results and Analysis

3.1 Composition and thermal activation of raw kaolin

The main chemical composition of Hainan kaolin is shown in Table 1. The content of burning base Al2O3 is 38.58%, which is slightly lower than the content 45.94% of theoretically pure kaolin (Al2O3·2SiO2·2H2O), but is similar to that of S2-16, a typical commercial industrial kaolin.

Table 1 Composition content of kaolin/%

Kaolin		Al_2O_3	Fe_2O_3	SiO_2	K_2O	Na_2O	ignition loss
HN19 kaolin	dry base	33.42	0.52	40.23	1.08	0.14	13.37
	burning base	38.58	0.60	46.44	1.25	0.16	0.00
Typical industrial kaolin (S2-16)	dry base	33.25	0.62	51.27	0.43	0.59	13.49
	burning base	38.43	0.72	59.26	0.50	0.68	0.00
Theoretical kaolin	dry base	39.53	0.00	46.51	0.00	0.00	13.95
	burning base	45.94	0.00	54.05	0.00	0.00	0.00

To improve the leaching rate of aluminum salt extracted from Hainan kaolin by acid method, this paper uses calcination method to activate Hainan kaolin [13,14] and investigates the effect of activation temperature on the leaching rate. Figure 1 is the thermogravimetric-differential thermal curve of HN19 kaolin. Seen from the TG curve, when the temperature is between 454.36℃─622.35℃, the mass fraction of kaolin decreases sharply, and its characteristic endothermic peak value is 502.35℃. At this stage, kaolin loses its bound water and gradually changes into metakaolin. DSC curve also has an exothermic peak at 990℃ when the crystal form gradually changes into mullite. Therefore, the thermal activation temperature of the primary selected kaolin was investigated in the range of 700℃-900℃. It can be seen from Figure 2 that as the calcination temperature increases, the leaching rate of activated alumina first increases and then decreases. For its reason, as the calcination temperature increases, the kaolin structure collapses and the activity increases. When the temperature further increases, the kaolin crystal form changes with activity decreased [15]. When the activation temperature is 800°C, the alumina leaching rate is the highest, so the calcination activation temperature of kaolin is selected as 800°C.

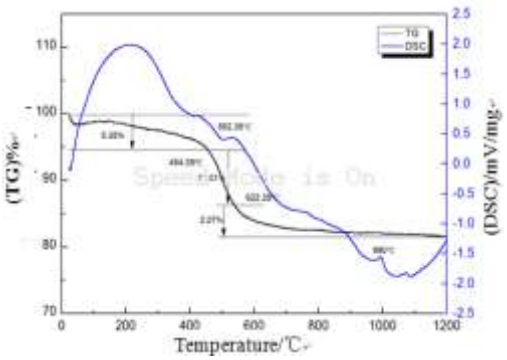

Fig 1: Kaolin thermogravimetry-differential thermal curve

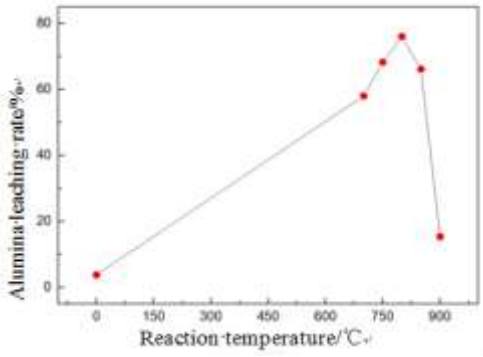

Fig 2: The relationship between kaolin activation temperature and leaching rate

3.2 Leaching process optimization for kaolin Al2O3

There are three major processes for extracting alumina from kaolin, namely Bayer method, acid method and sintering method [11]. Hydrochloric acid method is simpler than the Bayer method and the sintering method in aluminum salt extraction, the leaching rate is higher, and aluminum chloride can be directly used as the aluminum source for preparing Al2O3 after impurities removal through salt precipitation[11,16]. Due to kaolin of different mineral sources, there are big differences in the highest acid leaching rate of Al2O3 and the acid leaching conditions. Accordingly, this paper uses the uniform design WUST method to design the U12(12^6) test plan (Table 2) to

optimize the process parameters. The maximum and minimum values of the variables in Table 2 are determined based on the results of single factor experiments. According to the experimental data No. 1-12 in Table 2, the quadratic regression equation is established:

$$Y = -198.06 + 5.75X_5 + 0.0276X_1X_4 - 0.0282X_1X_5 - 0.017X_3^2 + 0.017X_3X_4 + 0.022X_3X_6 - 0.0037X_4X_5 - 0.036X_4X_6 - 0.023X_5^2 + 0.014X_5X_6 \quad (1)$$

When the confidence level of this equation is a=0.01, the multiple correlation coefficient F=0.9999, and the remaining standard deviation S=9.2×10-3, which indicates that the regression equation is highly reliable. WUST5.0 software was used to optimize the prediction, and three leaching experiments were performed under optimized process conditions (see Table 2). The average leaching rate was 97.9%, which was close to the predicted value99.0% of the regression equation, and the relative error was 1.11 %, indicating that the optimization process is reliable and can be used as the process conditions for acid leaching of alumina from Hainan kaolin.

Table 2 Uniform design test plan for alumina leaching and its test results

Experiment	HCl concentration X_1 /%	leaching temperature X_3/℃	leaching time X_2/h	solid/liquid X_4/mL•g^{-1}	HCl flushing dose/solid X_5/mL•g^{-1}	HCl mass concentration X_6/%	Al_2O_3 leaching rate Y/%
1	15	50	1.5	4	2	15	69.9
2	35	155	3.5	4	1	10	90.1
3	30	80	1.5	1	5	15	82.3
4	35	65	0.5	2	1	5	77.0
5	15	170	2.5	1	2	10	82.4
6	20	50	0.5	5	1	5	83.3
7	20	95	1.5	3	4	15	87.3
8	20	140	2.5	5	2	5	94.6
9	15	185	3.5	2	5	5	88.0
10	25	125	0.5	3	4	10	89.2
11	25	110	4.5	2	3	15	85.6
12	30	65	4.5	1	3	10	77.4
Optimization	15	183	0.5	5	4.98	5	97.9

3.3 Preparation of submicron spherical alumina

3.3.1 Research on the influence of dispersant on the morphology of alumina particles

Considering that traditional uniform precipitation method generally has problems such as a wide distribution range of sample particle size, serious particle agglomeration and low sphericity, in this experiment, dispersant was added to the reaction system for regulation. The experimental results are shown in Table 3 and Figure 3.

It can be seen from Table 3 that the dispersant exerts no effect on the primary particles (XRD particles) of Al2O3, which are all 35nm, but there is great influence on the secondary particles (SEM particles) and agglomerate particles (Laser particles). In terms of operational performance of alumina [17], its impact on electronic materials is mainly reflected in the size and morphological characteristics of secondary particles, followed by aggregate particles. It can be seen from Table 3 that, Al2O3 powder prepared by purified alginate AG has smaller secondary particles and agglomerate particles than other surfactants. Seen from SEM in Figure 3, the outstanding advantage of AG dispersion method lies in the good uniformity of the prepared spherical Al2O3 particles, indicating that purified Danish agar AG is a good dispersant for preparing spherical alumina.

Table 3 The influence of different dispersants on particle size

Dispersant	primary particle size (XRD particle size) /nm	secondary particle size (SEM particle size) /μm	Aggregate scattering particle sizeD_{50} (Laser particle size) /μm
None	35.8	~0.1-3.9	14.55
hexadecyl trimethyl ammonium bromide	35.5	~1.0-4.2	7.760
polyvinylpyrrolidone	35.7	~2.0-4.0	6.547
sodium dodecyl benzene sulfonate	35.3	~0.3-5.0	16.30
Sodium oleate	35.6	~0.4-1.5	8.327
Purified algin (AG)	35.7	~0.3-0.5	2.697

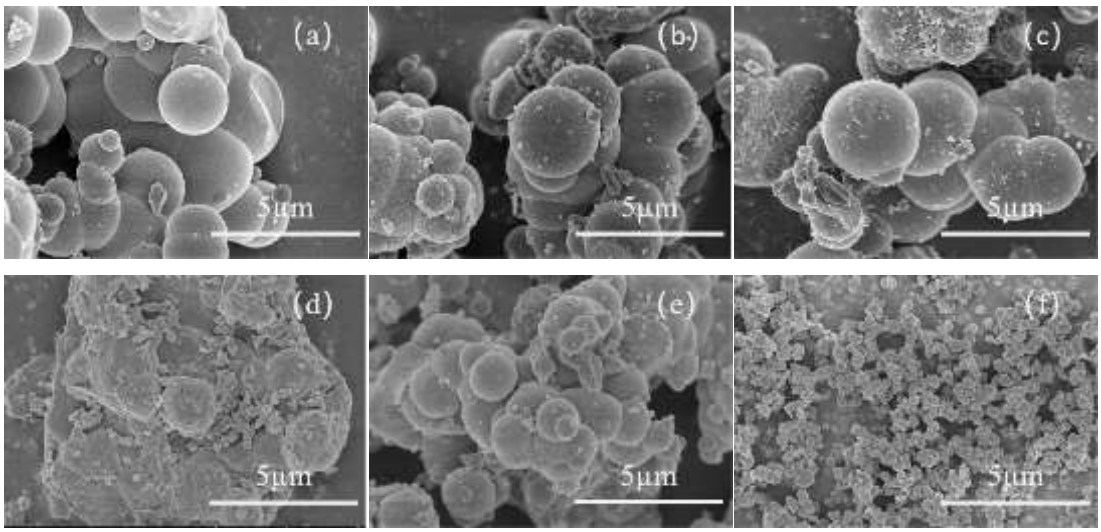

Fig 3: Effect of different dispersants on particle size and its dispersion
(a) None; (b) hexadecyl trimethyl ammonium bromide; (c) Polyvinylpyrrolidone; (d) sodium dodecyl benzene sulfonate; (e) Sodium oleate; (f) AG

3.3.2 Effect of preparation process conditions on alumina particle size

In addition to the vital role of the dispersant, other preparation process conditions are also important factors affecting the characteristics of alumina particles. These factors include reaction temperature, reaction time, precipitation dose (urea/aluminum ratio), and AG addition amount. Considering the possible interaction between these factors, the orthogonal design experiment L9(34) was carried out on the basis of single factor experiment to optimize the preparation process parameters. The factor level design of the orthogonal experiment is shown in Table 4. The level range of each factor is determined based on the previous single factor experiment. Take the laser particle size D50 of the prepared alumina as the target value, then the orthogonal experiment results are shown in Table 5, and the factor effect analysis results are shown in Figure 4.

Table 4 Factor level design table for orthogonal experiment

number of clustering.	Temperature/℃	Time/h	Urea/Aluminum/(n/n)	AG/%
1	105	8	8	0.75%
2	110	9	10	1.00%

3	115	10	12	2.00%

Table 5 Orthogonal experiment results and visual analysis

Experiment	Temperature/℃	Time/h	Urea/Aluminum/(n/n)	AG/%	Aggregate scattering particle sizeD_{50}/μm
1	105	8	8	0.75	5.987
2	105	9	10	1.00	3.069
3	105	10	12	2.00	7.417
4	110	8	10	2.00	4.053
5	110	9	12	0.75	2.816
6	110	10	8	1.00	3.921
7	115	8	12	1.00	3.525
8	115	9	8	2.00	1.638
9	115	10	10	0.75	2.952
Direct analysis result:					
Mean 1	5.491	4.522	3.849	3.918	--
Mean 2	3.597	2.508	3.358	3.505	--
Mean 3	2.705	4.763	4.586	4.369	--
extremely poor	2.786	2.255	1.228	0.864	--

From the orthogonal experiment and visual analysis results in Table 3, it can be seen that among the range values of various factors, the range of temperature factor is the largest, and that of AG is the smallest, indicating that AG amount exerts the least influence on particle size, while temperature difference has the largest influence.

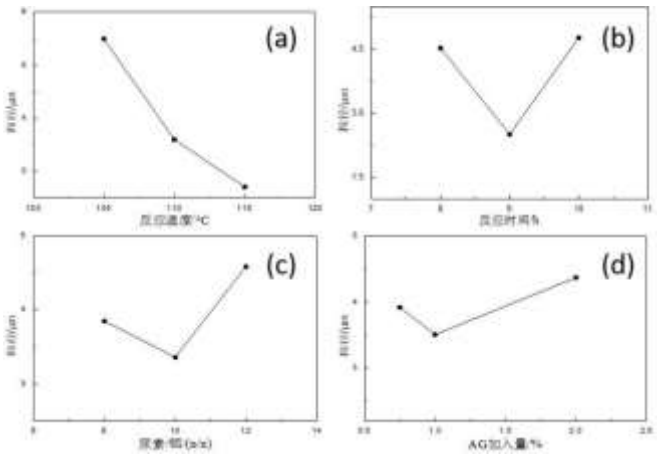

Fig 4: Factor-effect analysis diagram of orthogonal design experiment
(a) Temperature-particle size effect diagram; (b) Reaction time-particle size effect diagram; (c) Urea/aluminum-particle size effect diagram; (d) AG addition amount-particle size effect diagram

It can be seen from the factor effect analysis diagram in Figure 4 that, after considering the interaction effects of various factors, the optimized process conditions are reaction temperature 115℃, reaction time 9h, urea/aluminum ratio (n/n) 10, alginate addition amount 1.0%.

3.3.3 Performance of spherical submicron alumina

On the basis of the aforementioned optimization process, with Hainan kaolin as raw material, spherical submicron alumina powder QNA was prepared by the AG dispersion method under optimized process conditions, and its particle characteristics were analyzed and characterized, with results shown in Figure 5-7.

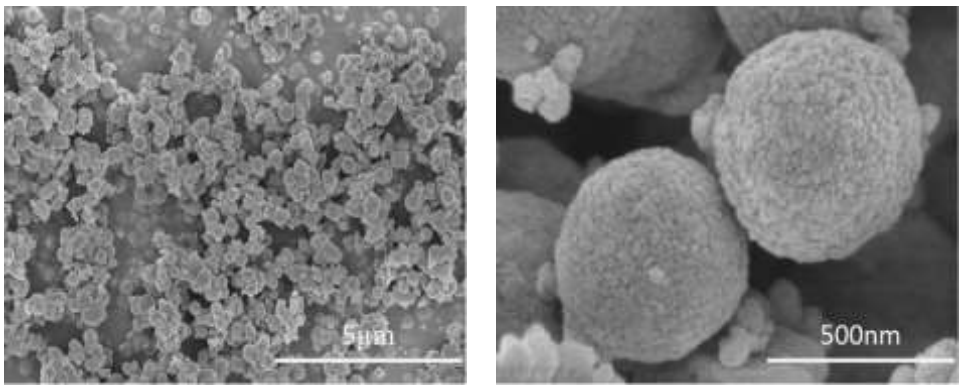

Fig 5: SEM image of QNA alumina

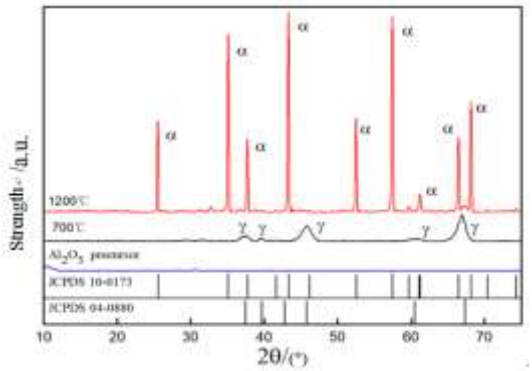

Fig 6: XRD spectrum of QNA alumina

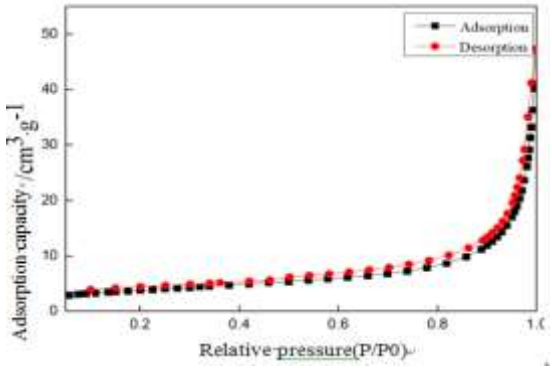

Fig 7: BET adsorption curve of QNA alumina

Figure 5 shows that by using AG dispersion method and optimized process, it is possible to prepare spherical submicron alumina with good circularity, low inter-particle adhesion, high particle uniformity, and SEM particle size of about 350nm.

The XRD phase analysis in Figure 6 shows that the spherical submicron alumina QNA powder is in α phase with no other impurity crystals, which is an ideal raw material for the production of lithium battery anode [17].

The N2-BET analysis in Figure 7 shows that the adsorption curve almost overlaps with desorption curve. BET has no obvious hysteresis loop of adsorption-desorption curve. The powder has uniform packing pores and regular powder pore structure, and there is no "ink bottle configuration hole", which indirectly proves concentrated particle size distribution in the powder (that is, the particle size is uniform) [18].

3.3.4 Discussion on the Dispersion Mechanism of Danish agar AG

The molecular structure of Danish agar AG is a double helix structure formed by hydrogen bond interaction of the linear chain composed of D-galactose and 3,6-anhydro-L-galactose, and there is hydroxyl free H+ on the main chain [19- 20]. There is active -OH on the surface of Al2O3 particles produced by uniform precipitation of urea [21]. The two usually undergo dehydration condensation reaction to form AG polymer [22]:

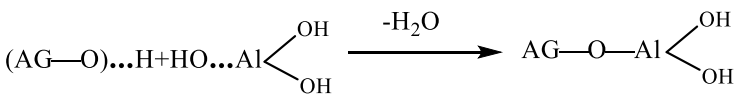

Since AG is attached to the surface of Al2O3 particles, the agglomeration between Al2O3 particles is hindered. These dispersed particles are then freeze-dried, thermally dried, and calcined to form dispersed spherical submicron alumina (Figure 8).

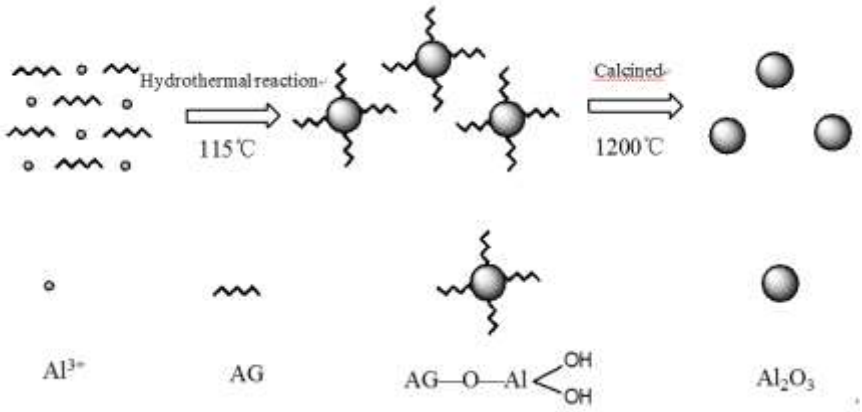

Fig 8: Schematic diagram of AG dispersion

IV. Conclusion

The acid extraction of alumina in kaolin HN19 is explored. The composition analysis shows that Hainan kaolin HN19 has a high alumina content of more than 38%; after the optimization by acid leaching process, the alumina extraction rate is as high as 97%, so kaolin HN19 can be used as a mineral source for extracting alumina.

Preparation of spherical submicron alumina by dispersant method is explored. After the aluminum salt obtained by acid leaching of kaolin HN19 was treated by salt precipitation to remove purities, method of using purified alginate AG as the dispersant to prepare spherical submicron alumina is studied. After process optimization, α-Al2O3 powder with good sphericity, good uniform dispersion and an average particle size of about 350nm was prepared.

Acknowledgements

Fund Project: Horizontal Project of Hainan University (HD-KYH-2014003).

References

[1] P.Y. An. “Review and forecast of alumina market analysis,” Light Metals, vol., no. 5, pp. 1-6, 2019.
[2] S.L. Zhang. “China's bauxite import demand remains strong,” Maritime China, vol. 12, pp. 78-80, 2018.
[3] Wiewiorowski T K & Miller D.J. Production of alumina from ores, U.S 3961030, 1976-06-01
[4] X.B. Li, H.Y. Wang, Q.S. Zhou, et al. “Efficient separation of alumina and silica in reduction-roasted kaolin by alkali leaching,” Trans. Nonferrous Met. Soc. of China, vol 29, no. 2, pp. 416-423, 2019.
[5] Y.C. Fu. “Technical analysis on nano-alumina preparation from kaolin,” China High Technology Enterprises, vol. 04, pp. 69-70, 2016.
[6] Losic D, Santos A. Nanoporous Alumina-Fabrication, Structure, Properties and Applications, 2015,NY: Springer
[7] Myung S T, Izumi Komaba K,S, Sun Y K.et al. Role of Alumina Coating on LiNiCoMnO Particles as Positive Electrode Material for Lithium-Ion Batteries. Chem. Mater. vol. 17, no. 14, pp. 3695–3704, 2005.
[8] M.Z. Liu. “Synthesis and characterization of alumina micro-nano materials.” Changsha: Central South University, 2011.
[9] M.Q. Zhu. “Preparation and modification of ultrafine alumina,” Beijing: Beijing University of Chemical Technology, 2013.
[10] T. Yan. “Preparation of nano-alumina and its hollow alumina spheres,” Nanjing: Nanjing University of Science and Technology, 2016.
[11] T. Xu, H.P. Lan, C. Yang, et al. “Extraction of alumina from fly ash by grinding acid leaching-hydrogen

chloride bubbling crystallization," Inorganic Chemicals Industry, vol. 50, no. 1, pp. 57-61, 2018.
[12] Z.W. Li, A. Tian, Z.F. Wang, et al. "Preparation of high-purity monodisperse spherical nano-alumina from fly ash," Bulletin of the Chinese Ceramic Society, vol. 39, no. 3, pp. 812-818, 2020.
[13] J.C. Jian, Z. Liu, L.Y. Lai et al. "Research on the calcination and activation process of kaolin," China Powder Science and Technology, vol. 21, no. 1, pp. 52-57, 2015.
[14] Liew Y M, Kamarudin H, Al Bakri A M M, et al. "Optimization of solids-to-liquid and alkali activator ratios of calcined kaolin geopolymeric powder," Construction and Building Materials, vol. 37, pp. 440-451, 2012.
[15] Y.M. Zhang, C.R. Xiong. "A new way to enhance the porosity and Y-faujasite percentage of in situ crystallized FCC catalyst ," Catal. Sci. Technol., vol. 2, pp. 606-612, 2012.
[16] Al-zahrani A A, Abdul-majid M H. "Extraction of Alumina From Local Clays By Hydrochloric Acid Process," Eng Sci, vol. 20, no. 2, pp. 29-41, 2009.
[17] Y.H. Wang. The effect of phosphorus doping on the performance and structure of activated alumina and its mechanism. Tianjin: Tianjin University, 2008.
[18] K.J. Zhen. Basics of Catalysis (Third Edition). Beijing: Science Press, pp. 39-59, 2005.
[19] C. Hu, W. Lu, A. Mata, et al. "Ions-induced gelation of alginate: Mechanisms and applications," International Journal of Biological Macromolecules, 2021.
[20] S.L. Liu, F. Zhu, S.N. Lin, et al. "Study on the strength and relaxation characteristics of agar gel,". Science and Technology of Food Industry, vol. 38, no. 13, pp. 85-89+100, 2017.
[21] K.FukushI, K.Tsukimura, H.Yamada. "Surface acidity of amorphous aluminum hydroxide," Acta Geologica Sinica, vol. 4, pp. 616, 2006.
[22] D.W. Zhu, D.S. Cheng, M.J. Geng, et al. "Analysis on the structure of boron adsorption complex on the aluminum hydroxide surface," Journal of Huazhong Agricultural University, vol. 1, pp, 3-5, 1998.